Cyanobacterial stabilized phycobilisomes as fluorochromes for extracellular antigen detection by flow cytometry

William G. Telford [a,*], Mark W. Moss [b], John P. Morseman [b], F.C. Thomas Allnutt [b]

[a] *Department of Experimental Transplantation and Immunology, Medicine Branch, Division of Clinical Sciences, NCI-NIH, Bethesda, MD, USA*
[b] *Martek Biosciences Corporation, Columbia, MD, USA*

Abstract

Phycobilisomes are cyanobacterial photosynthetic energy transfer complexes partly composed of phycobiliproteins, proteins that are widely used as conjugable fluorochromes for flow cytometry. The brightness and photostability of phycobiliproteins suggest that intact phycobilisomes could constitute even brighter probes for fluorescence-based detection systems. Stabilized phycobilisomes have been isolated and the red-excited, far red-emitting *Spirulina platensis*-derived complex PBXL-3 was accessed as a fluorochrome for flow cytometric immunodetection of surface antigens on immune cells. Although the large size of intact phycobilisomes initially precluded efficient cell surface labeling, the addition of a PEG spacer arm between PBXL-3 and its conjugated avidin molecule (designated PBXL-3L) reduced the steric hindrance associated with the high molecular weight PBXL complex. PBXL-3L increased the surface labeling surface-to-noise ratio and subsequent sensitivity by several-fold over commonly used red-excited fluorochromes such as APC. Interestingly, low power laser sources (including helium–neon and red diode) were particularly efficient at exciting PBXL-3. PBXL-3 was also compatible in with other fluorochromes for multicolor flow cytometry applications. In summary, PBXL-3 was found to possess superior sensitivity and efficiency for flow cytometric immunodetection, particularly with low power laser sources. © 2001 Elsevier Science B.V. All rights reserved.

Keywords: Cyanobacteria; Phycobiliprotein; Phycobilisome; Flow cytometry

1. Introduction

Phycobilisomes are supramolecular energy transfer complexes produced by red or blue-green cyanobacteria (Gannt and Lipschultz, 1972; Gannt et al., 1979; Yakamura et al., 1980; Glazer, 1984; MacColl and Guard-Friar, 1987). Phycobilisomes are composed of several types of phycobiliproteins and colorless polypeptides assembled in specific configurations for optimized energy transfer to downstream photosynthetic complexes (Gantt and Lipschultz, 1973; Gagliano et al., 1985; Biggins and Bruce, 1989; Brimble and Bruce, 1989). Phycobilisomes are the natural source of the phycobiliproteins phycoerythrin (PE) and allophycocyanin (APC). These dyes are widely used as labeling reagents for a variety of

---

fluorescence detection applications, including flow cytometry (Oi et al., 1982; Yeh et al., 1987).

The complicated subunit structure of phycobilisomes gives them unique fluorescent properties that are dependent on each phycobilisome type's component phycobiliproteins, chromophores and linker proteins. For example, the phycobilisome of the cyanobacterium *Arthrospira platensis* (a.k.a. *Spirulina platensis*) is composed of allophycocyanin (APC) and C-phycocyanin (C-PC) (Zhang et al., 1999). The C-PC is stacked (by association with specific colorless polypeptides) in rod-like structures that are positioned on the outer regions of the phycobilisome. These C-PC-containing rods are attached by one end to a stack of three APC-containing rods, called the core, which make up the center of the phycobilisome. The APC-rich phycobilisome core is then attached to a photosynthetic membrane for light energy capture by photosynthetic cells. APC is connected to the Photosystem II photosynthetic complex via a linker polypeptide that contains a chromophore, allowing the efficient transfer of light energy to chlorophyll.

Synthetic energy transfer complexes between phycobiliproteins and low molecular weight synthetic fluorochromes, including PE-Cy5, PE-Cy7 and APC-Cy7, are commonly used in flow cytometry. These tandem conjugates fluoresce at longer wavelengths than phycobiliproteins alone, thereby broadening the selection of compatible dyes for multicolor flow cytometry (Glazer and Stryer, 1983; Landsdorp et al., 1991; Waggoner et al., 1993; Beavis and Pennline, 1996; Roederer et al., 1996). Nevertheless, the resonance energy transfer in these complexes is generally inefficient and difficult to replicate from synthesis to synthesis. In contrast, the phycobilisome is optimized by nature to be extremely efficient in energy transfer. The use of phycobilisomes as fluorescent labels is an intriguing prospect, since the intact complex constitutes a large and naturally occurring energy transfer complex. Such a structure would be predicted to have far greater fluorescence intensity per binding event than a single phycobiliprotein. The phycobilisome would also have unique excitation/emission properties; for example, an R-PE/C-PC/APC phycobilisome could be excited with a 488 nm laser and then emit in the red

(666 nm), making it potentially useful for multicolor flow cytometry with FITC and PE.

Recently, the chemical stabilization of isolated intact phycobilisomes was reported (Cubicciotti, 1997) and the use and optimization of these complexes for specific binding reactions is being actively explored by the authors. One chemically stabilized phycobilisome, designated PBXL-1, is isolated from the red alga *Porphyridium cruentum* and contains B-phycoerythrin (B-PE), R-phycocyanin (R-PC), and APC as its constituent fluorophores. PBXL-1 possesses an excitation maximum at 545 nm and an emission maximum at 666 nm, with several other excitation/emission peaks reflecting the subunit structure. PBXL-1 can be effectively excited with the 488 nm argon laser line found on most flow cytometers. A second chemically stabilized phycobilisome, designated PBXL-3, is derived from *A. platensis* (a.k.a. *S. platensis*) and is composed of C-PC and APC as described above. PBXL-3 possesses excitation and emission maxima at 614 nm and 662 nm, respectively. Both complexes are extremely large, with estimated molecular weights exceeding 10,000 kDa. PBXL complexes are highly stable in solution and can be readily conjugated to streptavidin. They have since found usage in several fluorescence detection systems, including microplate immunoassays, prompt fluorescence detection of proteins on membranes, and in the detection of single nucleotide polymorphisms (SNPs) on DNA microarrays (Zoha et al., 1998; Morseman et al., 1999, 2000). In all of these systems, the use of PBXL dyes as fluorochromes improved assay sensitivity by at least fivefold, reflecting the high fluorescence yield of these complexes.

However, early experiments with PBXL fluors for intact cell labeling for flow cytometry proved disappointing. Labeling intact cells with streptavidin-conjugated PBXL dyes or a single phycobiliprotein with similar excitation/emission characteristics (for example, PBXL-3 and APC) gave roughly equivalent detection sensitivity (Telford, Moss, Morseman and Allnutt, unpublished data). These results were unexpected, given the greater brightness of the PBXL-3 dye. One explanation for the observed results could be that the large size of the PBXL complex (50–80 nm) could sterically hinder reagent binding to intact

cells. PBXL–streptavidin conjugates have since been developed that interpose a polyethylene glycol (PEG) spacer arm between the PBXL complex and the binding moiety, to reduce possible steric hindrance. The PEG tethered PBXL-3–streptavidin conjugates (henceforth designated PBXL-3L) demonstrated improved complex binding to intact cells in microplate assays (unpublished data). The PEG tethers may also positively affect complex solubility and binding kinetics.

In this paper, we evaluated the utility of one streptavidin PEG tethered PBXL dye conjugate for the extracellular labeling of intact cells for flow cytometry, namely the *A. platensis* phycobilisome PBXL-3L. Since this complex has spectral properties similar to APC, we set out to determine whether it could serve as a more sensitive substitute for APC in both single and multicolor flow cytometric applications. We determined that the PBXL-3L complex did indeed produce brighter cell labeling than APC for flow cytometry, allowing the detection of weakly expressed cell surface markers. Additionally, the high fluorescense intensity of the PBXL-3L complex also makes it well suited for the low power laser sources becoming more common in flow cytometric analysis (Shapiro, 1995). Finally, PBXL-3L was found to be compatible with a variety of other common immunophenotyping fluorochromes, extending its utility to multicolor flow cytometry.

2. Materials and methods

2.1. Cells

Several cell types were used in these studies. The EL4 mouse cell line was obtained from the American Type Culture Collection (Manassas, VA) and serially passaged in RPMI 1640 with 10% fetal bovine serum (FBS). The EL4-SAM cell thymoma cell line was generously provided by Dr. A. Sapozhnikov (Moscow, Russia) and grown similarly to EL4. Human peripheral blood mononuclear cells (PBMCs) were obtained from fully informed and consenting donors by venipuncture and red blood cell (RBC) depleted by centrifugation over Ficoll-Hypaque (Amersham Pharmacia Biotech, Piscataway, NJ) sep-

aration gradients. Once harvested, cells were immunolabeled and washed at 4°C with phosphate buffered saline (PBS) containing 10 mM sodium phosphate (pH 7.0), 150 mM sodium chloride, 2% FBS and 0.1% sodium azide (henceforth termed label buffer). EL4 and EL4-SAM cells were labeled then washed in the label buffer without sodium azide, due to its toxicity to these cell lines.

2.2. Cell line immunolabeling

Harvested EL4 cells were subdivided into 12×75 mm culture tubes, washed with label buffer, decanted, then resuspended in one of the following biotinylated primary antibodies: anti-mouse CD95/Fas (clone Jo-2; BD Pharmingen, San Diego, CA), anti-mouse CD30 (clone mCD30.1, BD Pharmingen) or anti-mouse CD90/Thy1.2 (clone 5a-8; Caltag Laboratories, Burlingame, CA). Biotin-conjugated mouse, rat and hamster isotype control antibodies (BD Pharmingen) were used for all control samples. All primary antibodies were used at a concentration of approximately 2 µg/ml with 100 µl containing 1×10^6 cells per well. Cells were incubated for 30 min at 4°C, washed twice with label buffer, then resuspended in one of the following streptavidin–fluorochrome conjugates: FITC (Jackson Immunoresearch, West Grove, PA), R-PE (Caltag), PE-Cy5 (Caltag), PE-Cy7 (Caltag), APC (Caltag), APC-Cy7 (Caltag), stabilized lissamine rhodamine (Rhodamine Red X, Jackson ImmunoResearch), Alexa Fluor 568 dye (Molecular Probes, Eugene, OR), Alexa Fluor 594 dye (Molecular Probes), Texas Red (Molecular Probes), CryptoFluor-5 (Martek Biosciences, Columbia, MD), PBXL-3 or PBXL-3L (Martek Biosciences). Cells were generally labeled at 20 µg/ml fluorochrome–streptavidin conjugate final concentration, 100 µl volume per 1×10^6 cells unless otherwise noted. For comparative purposes, APC, PBXL-3 and PBXL-3L were all used at 20 µg/ml final concentration. For some experiments, mixtures of CD90-labeled EL4 cells labeled with different fluorochromes were prepared to test multicolor analysis compatibility.

The PBXL-3 labeled streptavidin was prepared by activation of the PBXL-3 with *N*-succinimidyl *S*-thioacetate (SATA; Pierce Chemical, Rockford, IL),

then deprotection with hydroxylamine to expose free sulfhydral groups that were then reacted with sulfosuccinimidyl 4-(N-maleimidomethyl)-cyclohexane-1-carboxylate (sulfo-SMCC; Pierce Chemical) to form a covalent bond between both components of the conjugate. The ratio of PBXL-3 to streptavidin was about 1:1. The improved PBXL-3 conjugates (PBXL-3L) utilized 2-iminothiolane or Traut's reagent as a cross-linker to activate the antibody. This was linked through a sulfhydral group to a maleimide on a PBXL-3 that had been modified at the amine groups using poly(ethyleneglycol)-α-N-hydroxysuccinimidyl proprionate, β-maleimide (Shearwater Polymers, Huntsville, AL). This cross-linking chemistry provided a much larger distance between the two components of the conjugate than the SATA/SMCC pair used previously. PBXL-3 streptavidin conjugates prepared in this manner remained stable in solution for up to 1 year at 4°C (data not shown). Preparation of antibody conjugates is currently in progress. Excitation/emission spectra were obtained with a Perkin Elmer Lambda 12 fluorescence spectrophotometer at $EX = 612$ nm for the emission curve and $EM = 662$ nm for the excitation curve (Fig. 1).
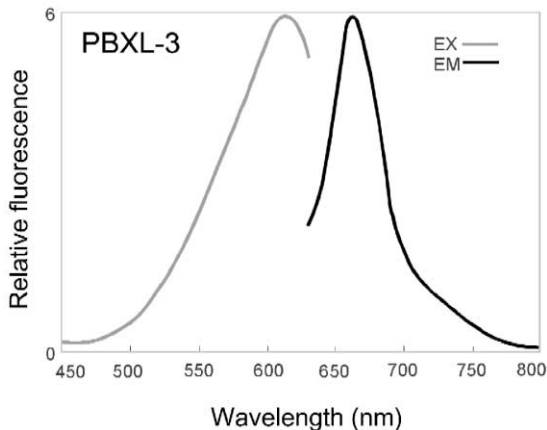

Fig. 1. Excitation/emission spectra for PBXL-3. Excitation (grey line) and emission (black line) for PBXL-3 in 0.75 M potassium phosphate pH 7.2. Excitation curve was measured at 662 nm emission, emission curve at 612 nm excitation. Curves are normalized for comparison purposes. The excitation and emission spectra for PBXL-3L were essentially indistinguishable from PBXL-3.

2.3. Peripheral blood mononuclear cell immunolabeling

PBMCs were prepared as above and simultaneously labeled with FITC-conjugated anti-human CD8 and PE-conjugated anti-human CD4. Cells were then washed and labeled separately with one of the following tandem conjugate third antibodies: PE-Cy5-anti-human CD3, PE-Cy7-anti-CD19 (Caltag), PerCP-anti-human CD19 or PerCP-Cy5.5-anti-human CD20 (BD Biosciences, San Jose, CA). Cells were then washed and labeled with biotin-conjugated anti-human CD120a (tumor necrosis factor receptor type I), followed by either APC– or PBXL-3L–streptavidin at the concentration described above. Cells were washed, resuspended in cold PBS and analyzed within one hour. Although all data shown depicts unfixed tissue, fixation with paraformaldehyde up to 2% had a minimal quenching effect on PBXL-3 fluorescence (data not shown).

2.4. Flow cytometry

The utility of PBXL-3L as a phenotyping fluorochrome was evaluated using a variety of instruments and laser sources. These are described below grouped by laser and excitation wavelength.

2.4.1. HeNe 632 nm and Kr 568 nm

A FACSVantage SE cell sorter (BD Biosciences) equipped with a I-90 water-cooled argon-ion laser (Coherent, Santa Clara, CA) emitting at 488 nm (150 mW), an I-302 water-cooled krypton-ion laser (Coherent) emitting at 568 nm (35 mW) and a helium–neon laser (Spectra-Physics, Mountain View, CA) emitting at 632 nm (35 mW) was used to evaluate PBXL-3L excitation/emission characteristics as a single color (Figs. 2–4), in four-color labeling combined with FITC, PE and APC-Cy7 (Fig. 7), and in two-color labeling combined with CryptoFluor-5, lissamine rhodamine, Alexa Fluor 568 dye or Alexa Fluor 594 dye (Fig. 8). All laser beams occupied spatially separated beam paths. Scatter measurements and instrument triggering were carried out using the argon-ion 488 nm laser. FITC and PE excited at 488 nm, with their signals separated using a 560 short pass (SP) dichroic and detected through 530 ± 30 and 575 ± 26 nm narrow band pass (NBD)

filters, respectively. PBXL-3 and PBXL-3L were excited with either the HeNe 632 nm or Kr 568 nm laser and detected through 660 ± 20, 675 ± 20, 682 ± 20 or 710 ± 20 nm NBP filters or 748 nm long band pass (LP) dichroic filters. APC and APC-Cy7 were excited using either HeNe 632 nm or Kr 568 nm lasers and detected through a 660 ± 20 nm NBP filter and 748 nm LP dichroic, respectively; their signals were separated using a 690 nm LP dichroic. CryptoFluor-5, lissamine rhodamine, Alexa Fluor 568 dye and Alexa Fluor 594 dye were excited with the Kr 568 nm laser and detected through a 610 ± 30 nm NBP filter; APC or PBXL-3L signals were separated from Texas Red or Alexa Fluor 594 dye using a 640 nm LP dichroic.

2.4.2. Red diode 635 nm

A FACSCalibur benchtop flow analyzer (BD Biosciences) equipped with an air-cooled argon-ion laser emitting at 488 nm (15 mW) and a red diode laser emitting at 635 nm (5 mW) was used to evaluate PBXL-3L excitation/emission characteristics alone (Fig. 3) and in four-color analysis with FITC, PE and PE-Cy5, PE-Cy7 or PerCP-Cy5.5 (Figs. 5 and 6). Scatter measurements and instrument triggering were carried out using the argon-ion 488 nm laser. FITC and PE excited at 488 nm, with their signals split using a 560 nm SP dichroic and detected through 530 ± 30 nm and 575 ± 26 nm NBD filters, respectively. PE-Cy5, PE-Cy7 and PerCP-Cy5.5 were excited at 488 nm, their signals separated from FITC and PE using a 610 nm SP dichroic and detected through a 650 nm LP dichroic. APC and PBXL-3L were excited with the red diode laser and detected though a 650 nm LP dichroic.

2.4.3. HeNe 594 and HeNe 612 nm

A customized hybrid FACS IV/FACStar cell sorter (BD Biosciences) equipped with either a helium–neon 594 nm laser (Melles Griot, Carlsbad, CA), 4.5 mW maximum power output) or a helium–neon 612 nm laser (Melles Griot, 4.5 mW) was used to evaluate PBXL-3L excitation/emission characteristics alone (Fig. 3), in three-color analysis with Texas Red or Alexa Fluor 594 and APC-Cy7 (Fig. 9, using 594 nm excitation) and in two-color analysis with APC-Cy7 (Fig. 10, using 612 nm excitation). Scatter measurements, instrument trig-

gering and fluorochrome excitation were all carried out using either the HeNe 594 nm or 612 nm laser in the primary position. APC and PBXL-3L were detected through a 660 ± 20 nm NBP filter. Texas Red and Alexa Fluor 594 dyes were detected through a 610 ± 30 nm NBP filter. APC-Cy7 was detected through a 748 nm LP dichroic. Texas Red and Alexa Fluor 594 dyes signals were split from the longer wavelength fluorochromes' signals using a 640 nm LP dichroic. APC or PBXL-3L and APC-Cy7 signals were split using a 690 nm LP dichroic.

2.4.4. Data acquisition and analysis

All comparison experiments were carried out on the same day using the same samples. All flow cytometry data were analyzed using CellQuest ver. 3.2 (BD Bioscience) and WinMDI ver. 2.8 (Dr. Joe Trotter, Scripps Institute) flow analysis software. Real-time hardware-based intra- and interlaser compensation was employed for all samples; relevant compensation percentages are indicated in the figures. Mean fluorescence intensity (MFI values) were used to gauge relative fluorochrome signal intensity; in some cases, ratios of specific and background MFIs (in boldface on figures) were used to compare fluorochrome brightness with differing excitation and emission detection conditions.

3. Results

3.1. Flow cytometric detection of cell surface antigens with PBXL-3 and PBXL-3L

The first goal of this study was to determine if PBXL-3 could be used as a immunophenotyping fluor for cell surface marker labeling, and whether its phycobiliprotein-rich structure rendered it brighter than existing red-excited fluorochromes (such as APC). The fluorescence excitation/emission spectra for PBXL-3 are shown in Fig. 1, as determined by fluorescence spectroscopy at 614 and 662 nm, respectively. The percentages of fluorescence relative to maximum efficiency at some common laser lines are shown in Table 1. These spectral characteristics indicated the probable need for an orange-red excitation source and a red emission filter for optimal measurement by flow cytometry. The initial testing

Table 1
Comparison of relative fluorescence intensity vs. the maximum achieved by excitation of PBXL-3 at 612 nm in 50 mM sodium phosphate (pH 7.2), 150 mM sodium chloride, and 0.05% sodium azide at various wavelengths corresponding to those utilized by the lasers indicated
Values are expressed as percentage of maximal emission at 662 nm.

Laser	Wavelength (nm)	Percentage of maximal
Red diode	635	84.7
Red helium neon	632	88.9
Orange helium neon	612	100
Yellow helium neon	594	87.1
Krypton-ion	568	54.4
Green helium neon	543	20.2
YAG	532	20.2
Argon-ion visible	488	30.1
Argon-ion UV	363	20.3
Krypton-ion UV	351	18.8

of PBXL-3 was therefore carried out on a FACSVantage SE cell sorter using a helium–neon (HeNe) laser emitting at 632 nm with 35 mW power output. Although not the optimal excitation wavelength for PBXL-3L, this laser type is commonly available on commercial flow cytometers and has a power output exceeding HeNe lasers with shorter wavelengths. A 660 ± 20 nm NBP emission filter was used for signal detection.

Murine EL4 cells were labeled with biotin-conjugated antibodies against three surface antigens: CD90 (strongly expressed on EL4 cells), CD30 (showing intermediate expression) and CD95 (weakly expressed). Cells were then secondarily labeled with streptavidin conjugated to one of four fluorochromes: FITC, APC, PBXL-3 (with no spacer arm) and PBXL-3L (with a PEG spacer arm insert between the fluor and the streptavidin). Cells were then analyzed using the above excitation/emission system. The results are shown in Fig. 2, with the mean fluorescence intensity (MFI) values for the background (open) and specific labeling (filled) peaks indicated and the ratio in boldface. The MFI ratio for FITC labeling (Fig. 2, row 1) was low, with CD95 expression being barely detectable. As expected, the situation improved with the phycobiliprotein APC labeling (Fig. 2, row 2), showing a 5- to 12-fold increase in sensitivity. Despite the expected bright-

ness of the PBXL-3 fluor (no spacer arm), it gave sensitivities equal to or somewhat below APC over a wide concentration range (Fig. 2, row 3). As discussed previously, the massive size of the complex may have hindered antibody binding. The addition of the PEG spacer arm between the fluor and the streptavidin (PBXL-3L) enhanced the binding efficiency and increased sensitivity up to five times greater than APC for all antigens tested (Fig. 2, row 4), evidence that steric hindrance with PBXL-3 conjugates could be the explanation for the suboptimal results with PBXL-3. CD95 expression, in particular, became well differentiated from background fluorescence with the PEG tethered PBXL-3L conjugate, in contrast to the other dyes tested (even to APC). PBXL-3L enhanced detection sensitivity of all three cell surface markers representing a broad range of expression levels. This demonstrates broad utility with special relevance to low density marker detection. Despite its large size, the addition of a PEG spacer arm made cell surface labeling with PBXL-3 feasible and delivers enhanced sensitivity compared to existing fluors.

3.2. PBXL-3L excitation characteristics

Although the HeNe 632 nm laser described above excited PBXL-3L with reasonable efficiency, the excitation spectrum for the fluor suggested that somewhat shorter wavelength sources might be even more effective. In fact, PBXL-3L may be well excited by wavelengths from a number of commercially available lasers. HeNe gas lasers can be built that generate lines at 594 and 612 nm, although these lasers are generally of low power (< 5 mW). Solid state diode lasers emit at 635 nm, 670 nm and at near infrared wavelengths at power levels up to 5 mW. The former of this group is now used in many benchtop flow cytometers for APC excitation and should excite PBXL-3L as well. More powerful krypton-ion gas lasers emit at 568 nm (yellow) and in the far red (647 nm) at levels exceeding 50 mW. Its 568 nm laser line, in particular, could also prove useful for PBXL-3L excitation.

To determine other useful laser wavelengths for PBXL-3L excitation, EL4 mouse thymoma cells were labeled with biotin-conjugated antibodies against the strongly expressed antigen CD90 as described above,
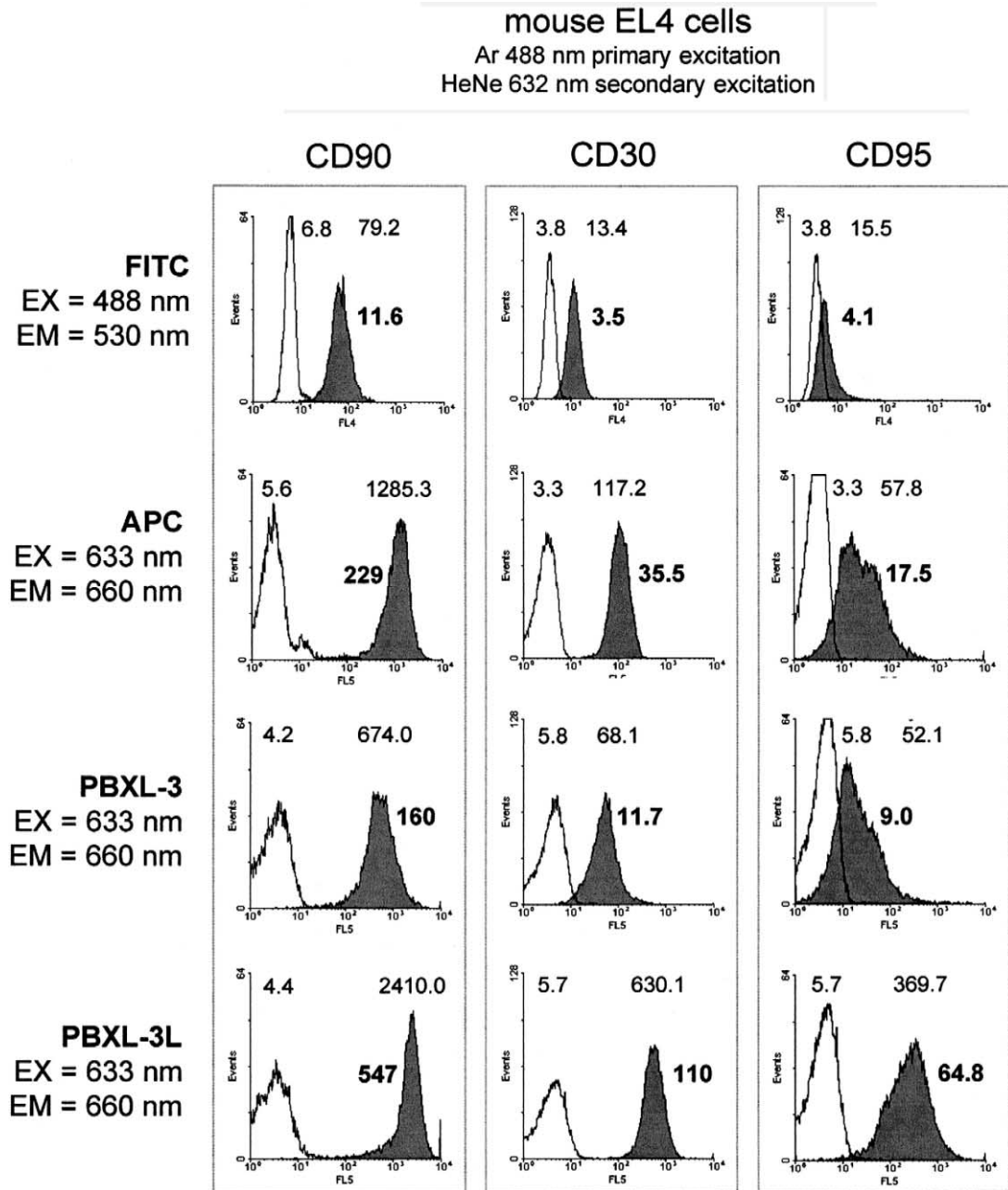
Fig. 2. Surface marker immunolabeling with APC and PBXL-3. EL4 cells were labeled with biotin-conjugated antibodies against mouse CD90, CD30 and CD95 (left, middle and right columns, respectively) followed by secondary labeling with streptavidin-conjugated to FITC, APC, PBXL-3 or PBXL-3L (rows 1, 2, 3 and 4, respectively). Excitation and emission wavelengths are shown next to each row. Mean fluorescescence intensity (MFI) values and their ratios (boldface) are shown for isotype control (open peaks) and specific labeling (filled peaks) on each histogram.

followed by streptavidin conjugated to PBXL-3L (or to APC for comparison purposes). Cells were analyzed using the lasers described above (HeNe 632 nm at 5 mW, red diode 635 nm at 5 mW, Kr 568 nm at 35 mW, HeNe 594 nm at 4.5 mW and HeNe 612 nm at 4.5 mW) on the instrument platforms described in Materials and methods. A 660 ± 20 nm NBP filter was used for PBXL-3L detection for all lasers except the red diode, where a 650 nm LP dichroic was used instead to minimize cross-talk. The results are shown in Fig. 3, with the MFI values for the background (open) and specific labeling (filled) peaks indicated and the s/n ratios in bold-face. Due to the different laser power levels and instrument platforms employed, it is difficult to draw precise conclusions from these comparisons. However, some general observations can be made. First, all laser sources tested excited PBXL-3L well, more than adequate for CD90 detection. Second, PBXL-3L labeling was brighter than APC for all laser sources, ranging from twofold brighter (HeNe 632 nm, 35 mW) to almost eightfold brighter (HeNe 594 nm, 4.5 mW and red diode 635 nm, 5 mW). Third, the signal-to-noise ratio for PBXL-3L labeling was more optimal for laser wavelengths approximating the excitation maxima as measured by fluorescence spectrophotometry (using the HeNe 594 nm and 612 nm lasers). Finally, the PBXL-3L signal to noise ratio was optimal using the lasers with the *lowest* power output (the HeNe 594 nm, HeNe 612 nm and red diode 635 nm). Thus, the red diode 635 nm laser, despite a predicted loss in excitation efficiency based on the excitation spectrum, gave a PBXL-3L signal to noise ratio stronger than shorter wavelength HeNe 594 and 612 nm lasers and greater than the more powerful HeNe 632 nm laser. This was in contrast to APC, which showed optimal excitation with the more powerful HeNe 632 nm laser and either equivalent or lower excitation with other lasers, including the red diode. The APC results (analyzed in the same experiments with PBXL-3L) also suggested that the greater efficiency of PBXL-3L with lower power laser sources was not due to instrument-specific trivial causes, such as the length of the laser path or differences in the emission filter. In summary, PBXL-3L efficiently detected a T cell surface antigen with superior brightness to APC. More surprisingly, however, PBXL-3L gave the strongest signal to noise ratio with low power lasers. This increased efficiency may make PBXL-3L more useful in instruments equipped with these excitation sources.

3.3. PBXL-3L emission characteristics

The predicted excitation maximum of PBXL-3L is in the 660–670 nm range, suggesting that filters appropriate for APC detection (such as a 660 ± 20 nm NBP filter) should be optimal for PBXL-3L as well. This was confirmed using the HeNe 632 nm laser as the excitation source and testing NBP filters and dichroics ranging from 660 to 748 nm (Fig. 4). As expected, a $660 + 20$ nm NBP filter was found to be optimal for PBXL-3L detection. However, reasonable levels of fluorescence could be detected beyond 700 nm. This was in contrast with APC, whose efficiency dropped significantly at this wavelength.

3.4. PBXL-3L in multicolor flow cytometry

A critical advantage of red-excited probes, such as APC, in flow cytometry is their ability to be combined with other fluorochromes for multicolor analysis using instruments with multiple lasers. The compatibility of APC with fluorochromes excited at other wavelengths (such as FITC, PE, PE-Cy5, etc.) has made possible the analysis of up to 12 fluorochromes simultaneously (Roederer et al., 1995, 1997). Simultaneous analysis of four to seven colors is now becoming routine on commercially available instruments. The importance of red-excited fluorochromes in multicolor analysis makes the compatibility of PBXL-3L a critical issue. The broad emission range of PBXL-3L over APC makes it necessary to test such compatibility and determine whether electronic and/or software compensation systems can correct for spectral overlap with other fluorochromes.

PBXL-3L labeling was therefore substituted for APC in several multicolor formats: (1) simultaneous analysis with three 488 nm-excited probes (FITC, PE, and several longer-wavelength tandem conjugates), (2) simultaneous analysis with other red-excited (632 nm) tandem conjugates, (3) simultaneous analysis with other yellow-excited (568 or 594 nm) fluorochromes and tandem conjugates, and (4) simul-
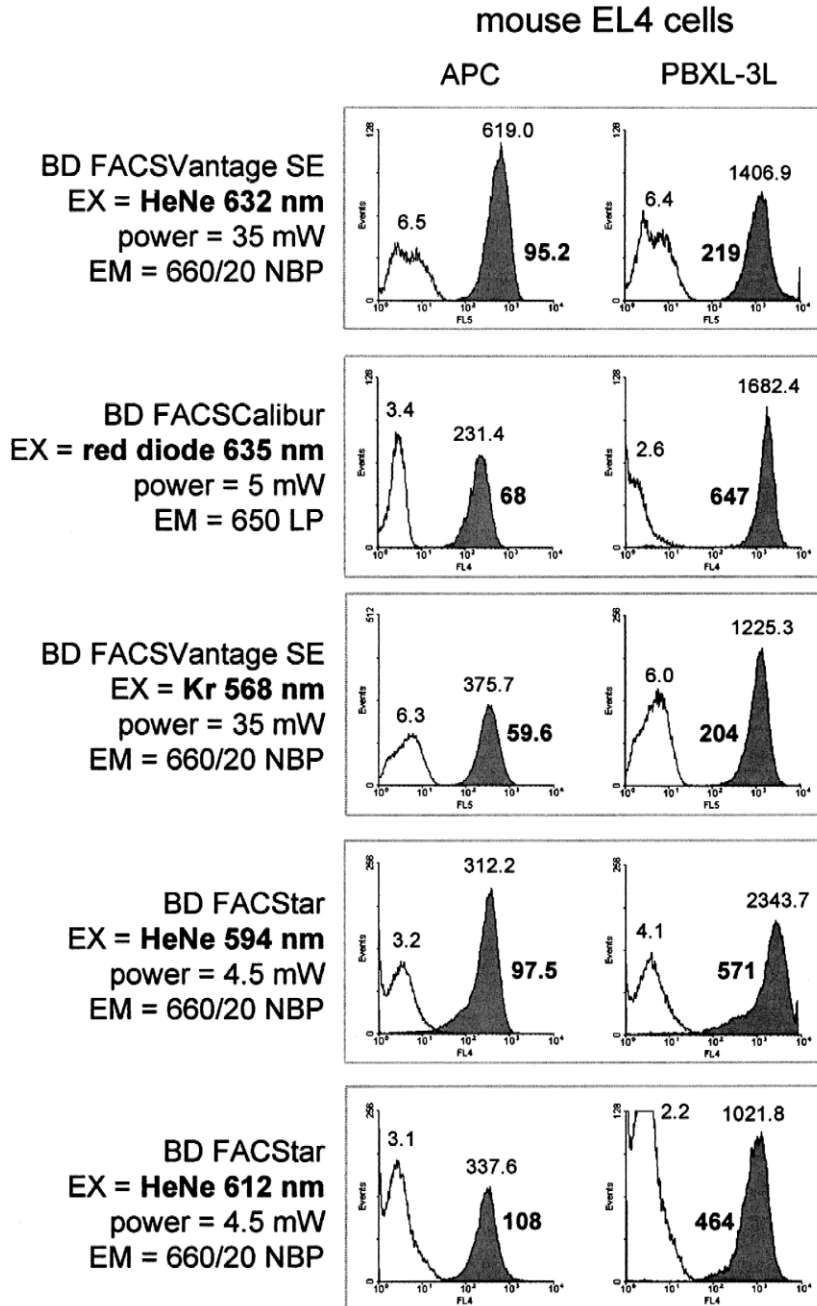
Fig. 3. Excitation sources for APC and PBXL-3L. EL4 cells were labeled with biotin-conjugated antibody against mouse CD90 followed by streptavidin-conjugated APC (left column) or PBXL-3L (right column). Cells were then analyzed on one of the following instrument-laser platforms: row 1, FACSVantage SE equipped with Ar 488 nm (150 mW) and HeNe 632 nm (35 mW) lasers; row 2, FACSCalibur with Ar 488 mW (15 mW) and red diode 635 nm (5 mW) lasers; row 3, FACSVantage SE with Ar 488 nm (150 mW) and Kr 568 nm (35 mW) lasers; row 4, hybrid FACStar with HeNe 594 nm (4.5 mW) laser; row 5, hybrid FACStar with HeNe 612 nm (4.5 mW) laser. Excitation and emission wavelengths are shown next to each row. Mean fluorescence intensity (MFI) values (over peaks) and their ratios (boldface) are shown for isotype control (open peaks) and specific labeling (filled peaks) on each histogram.
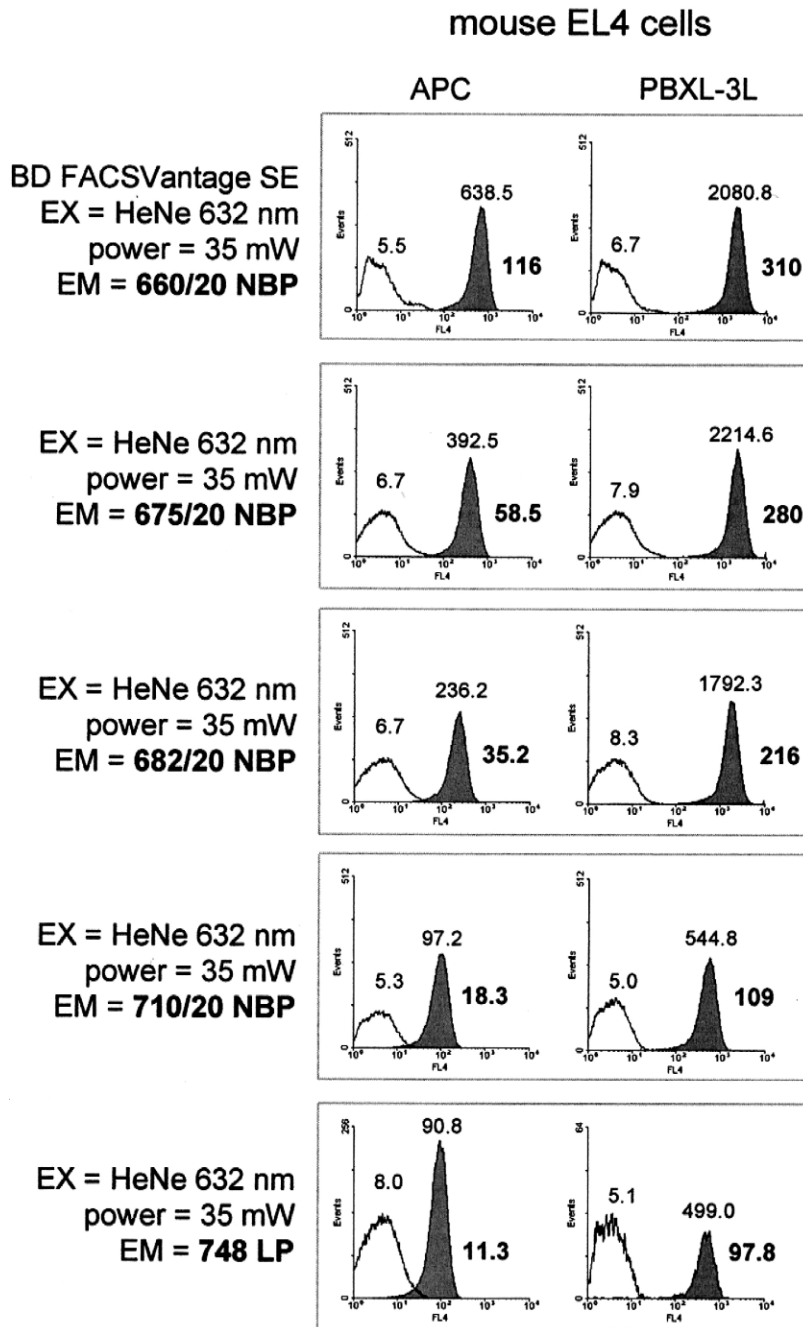
Fig. 4. Fluorescence emission of APC and PBXL-3L. EL4 cells were labeled with biotin-conjugated antibody against mouse CD90 followed by streptavidin-conjugated APC (left column) or PBXL-3L (right column). Cells were then analyzed on a FACSVantage SE equipped with Ar 488 nm (150 mW) and HeNe 632 nm (35 mW) lasers, with APC or PBXL-3L detection through 660 ± 20 nm NBP (row 1), 675 ± 20 NBP (row 2), 682 ± 20 nm NBP (row 3), 710 ± 20 nm NBP (row 4) or 748 nm LP filters or dichroic. Excitation and emission wavelengths are shown next to each row. Mean fluorescence intensity (MFI) values (over peaks) and their ratios (boldface) are shown for isotype control (open peaks) and specific labeling (filled peaks) on each histogram.

taneous analysis with other orange-excited (612 nm) tandem conjugates. Collectively, these results indicate that PBXL-3L is compatible with a variety of common phenotyping fluorochromes, subject to some additional color compensation.

The first scenario tested was human PBMCs labeled with FITC, PE and the far-red (710 nm) tandem conjugate PerCP-Cy5.5 conjugated to antibodies

against CD8, CD4 and CD19, respectively (Fig. 5). Cells were then labeled with biotin-conjugated antibodies against CD120a, the weakly expressed tumor necrosis factor type I receptor, followed by streptavidin conjugates of either APC (left panel) or PBXL-3L (right panel). Cells were then analyzed on a FACSCalibur with a red diode 635 nm laser. All two-color cytograms are shown, with the required
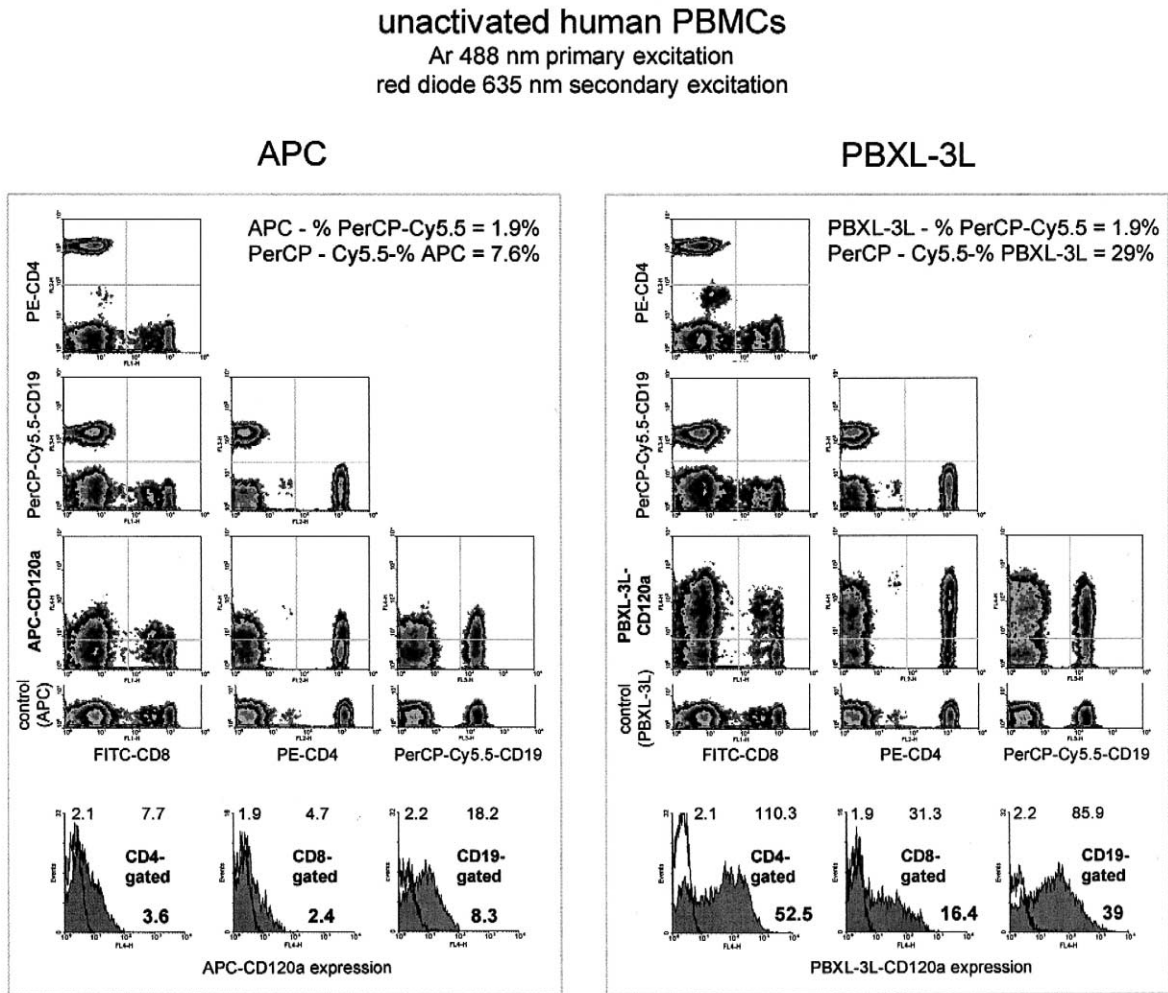

Fig. 5. Multicolor analysis with FITC, PE, PerCP-Cy5.5 and PBXL-3L. Human PBMCs were labeled with FITC-anti-CD8, PE-anti-CD4 and PerCP-anti-CD19, followed by biotin-anti-CD120a and streptavidin conjugated to either APC (left panel) or PBXL-3L (right panel). Cells were analyzed on a FACSCalibur equipped with Ar 488 nm (15 mW) and red diode 635 nm (5 mW) lasers. Data are displayed as cytograms with all two-color combinations, with color compensation percentages for APC or PBXL-3L and PerCP-Cy5.5 shown. Histograms at bottom show CD120a expression for CD4-, CD8- and CD19-gated fractions (left, middle and right histograms, respectively for each panel). Mean fluorescence intensity (MFI) values and the ratio of these values (bold type) are shown for isotype control (open peaks) and specific labeling (filled peaks) on each histogram.

compensation values between PerCP-Cy5.5 and APC or PBXL-3L given in the panel. PBXL-3L functioned well in this multicolor protocol, requiring no color compensation with FITC or PE. The compensation requirement for subtraction of PBXL-3L fluorescence from the PerCP-Cy5.5 signal was higher than APC, but was not excessive, being well within an acceptable range ($< 35\%$). As illustrated in the
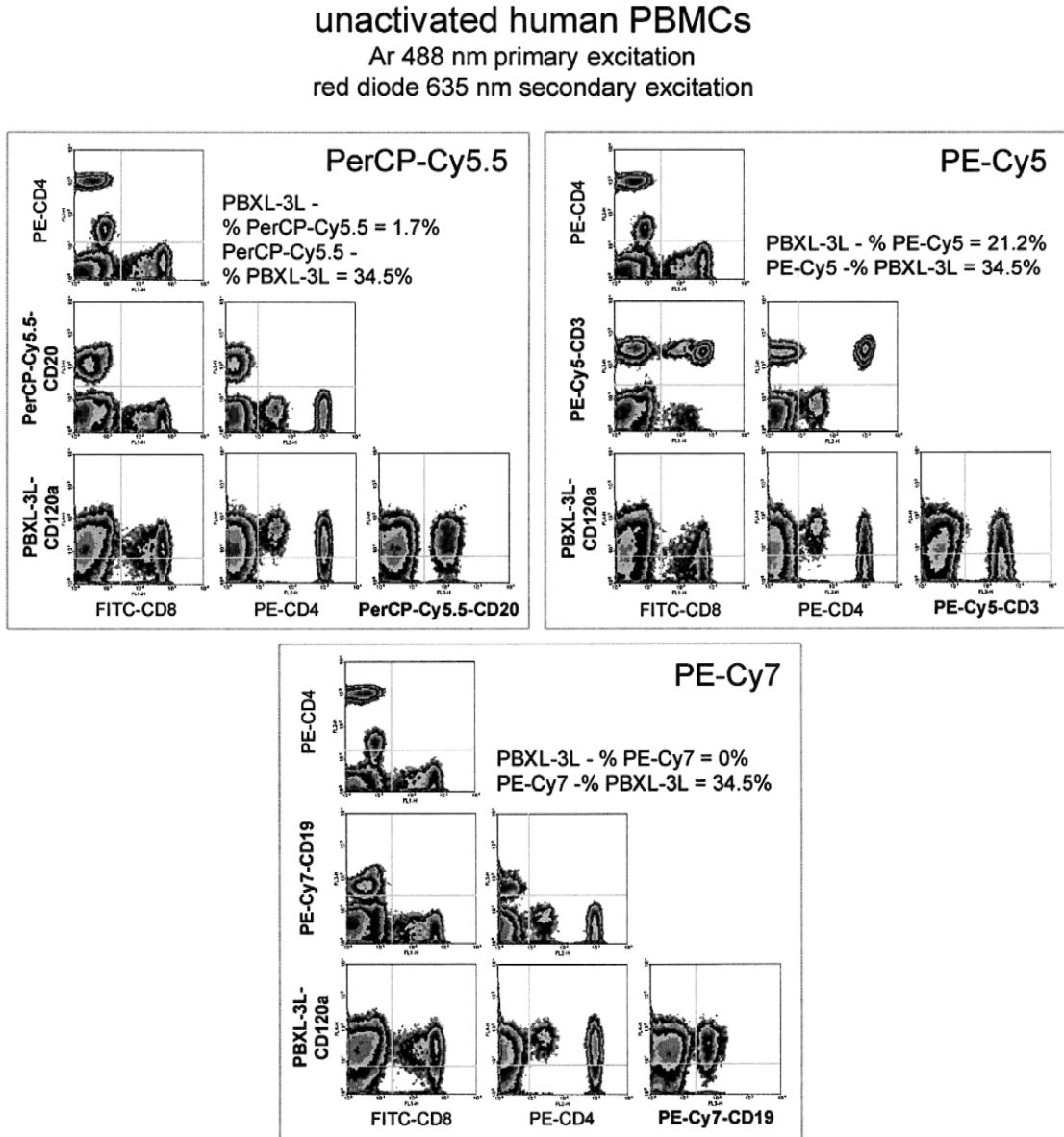

Fig. 6. Multicolor analysis with FITC, PE, PBXL-3L and PerCP-Cy5.5, PE-Cy5 or PE-Cy7. Human PBMCs were labeled with FITC-anti-CD8, PE-anti-CD4 and either PerCP-Cy5.5-anti-CD20 (top panel), PE-Cy5-anti-CD3 (middle panel) or PE-Cy7-anti-CD19 (bottom panel) followed by biotin-anti-CD120a and streptavidin conjugated to PBXL-3L. Cells were analyzed on a FACSCalibur equipped with Ar 488 nm (15 mW) and red diode 635 nm (5 mW) lasers. Data are displayed as cytograms with all two-color combinations, with color compensation percentages for APC or PBXL-3L and PerCP-Cy5.5, PE-Cy5 and PE-Cy7 shown.
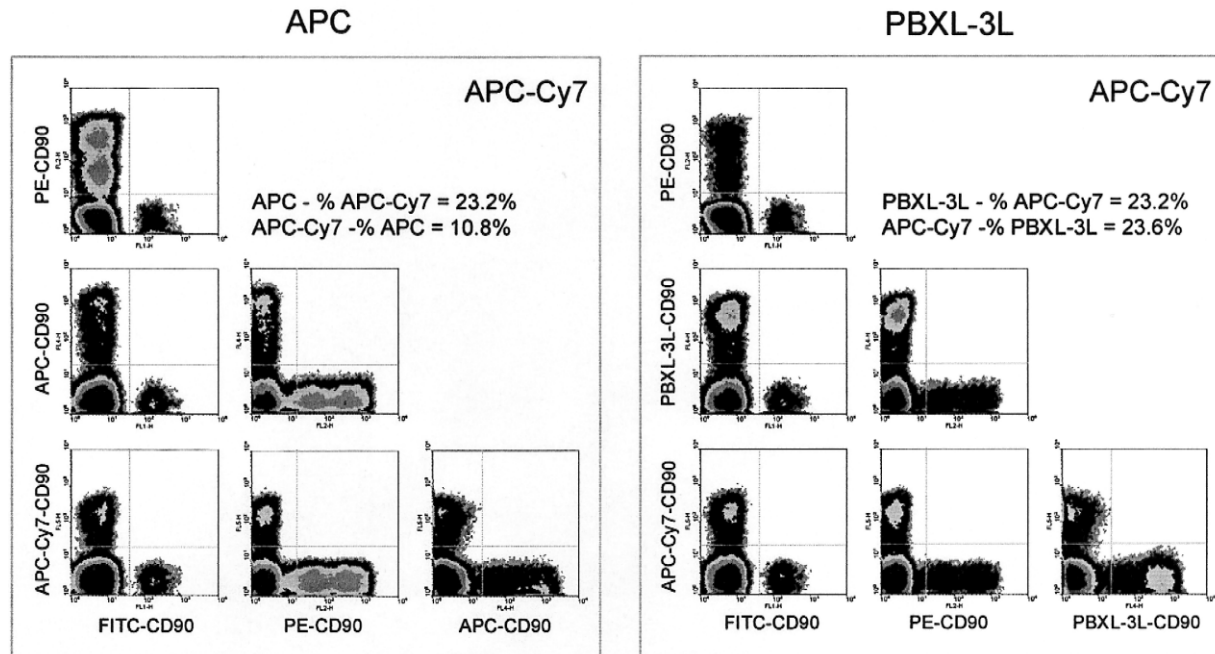
Fig. 7. Multicolor analysis with FITC, PE, APC-Cy7 and PBXL-3L. Mouse EL4-SAM cells were labeled with biotin-anti-CD90 followed by streptavidin conjugated with FITC, PE, APC, PBXL-3L or APC-Cy7. Labeled cells were then mixed in combinations of FITC, PE, APC and APC-Cy7 (left panel) or FITC, PE, PBXL-3L and APC-Cy7 (right panel) and analyzed on a FACSVantage SE equipped with Ar 488 nm (150 mW) and HeNe 632 nm (35 mW) lasers. Data are displayed as cytograms with all two-color combinations, with color compensation percentages for APC or PBXL-3L and APC-Cy7 shown.

CD4-, CD8- and CD19-gated histograms for CD120a expression below the cytograms, PBXL-3L increased sensitivity for the relatively weak CD120a expression by 4- to 10-fold, allowing clear delineation of antigen expression in the gated T and B cell subsets.

PBXL-3L also functioned well with other tandem conjugate dyes used in place of PerCP-Cy5.5. Fig. 6 shows PBMCs labeled in the same fashion but with adjustment in the 488 nm-excited far red tandem conjugate used; either PerCP-Cy5.5-anti-CD20 (top panel), PE-Cy5-anti-CD3 (middle panel), or PE-Cy7-anti-CD19 (bottom panel). PE-Cy5 emits at approximately 670 nm, while PE-Cy7 emits in the near infrared (750 nm). PBXL-3L was compatible with all

of these tandem conjugates, although a higher level of compensation and some loss of PBXL-3 signal was experienced with PE-Cy5 (similarly to what is normally seen with APC). Although the required subtraction of PBXL-3L signal from the PerCP-Cy5.5, PE-Cy5 and PE-Cy7 signal was again higher than APC, it was still within acceptable limits.

PBXL-3L was then tested with APC-Cy7, an APC tandem conjugate that excited in the red and emits in the near infrared (750 nm). Mouse EL4 cells were labeled with biotin-anti-CD90 followed by streptavidin conjugates of FITC, PE, APC or PBXL-3L and APC-Cy7. Mixtures of each single-labeled cell suspension and unlabeled cells were prepared
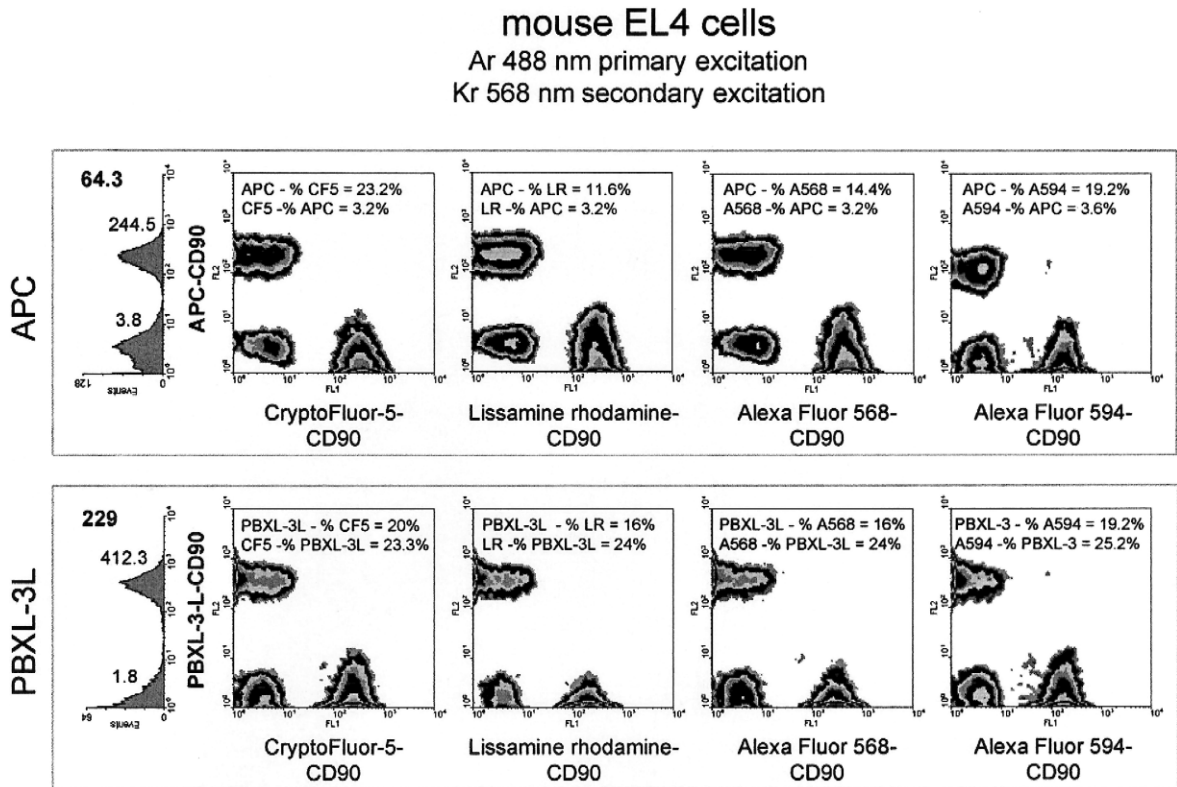

Fig. 8. Multicolor analysis with yellow 568 nm-excited probes and PBXL-3L. Mouse EL4 cells were labeled with biotin-anti-CD90 followed by streptavidin conjugated with either APC, PBXL-3L, CryptoFluor-5 (CF-5), lissamine rhodamine, Alexa Fluor 568 dye or Alexa Fluor 594 dye. Cell mixtures of APC (top row) or PBXL-3L (bottom row) and either CryptoFluor-5 (column 1 cytograms), lissamine rhodamine (column 2 cytograms), Alexa Fluor 568 dye (column 3 cytograms) or Alexa Fluor 594 dye (column 4 cytograms) were prepared and analyzed on a FACSVantage equipped with Ar 488 nm (150 mW) and Kr 568 nm (35 mW) lasers. Data are displayed as cytograms with all two-color combinations, with all color compensation percentages shown. APC and PBXL-3L labeling is shown in left-most histograms with mean fluorescence intensity (MFI) values and their ratios (boldface) shown for isotype control (open peaks) and specific labeling (filled peaks).

and analyzed on a FACSVantage SE with dual Ar 488 nm and HeNe 632 nm excitation. The results are shown in Fig. 7. The PBXL-3L signal could be satisfactorily separated from the APC-Cy7 signal using a 690 nm LP dichroic. Once again, somewhat higher color compensation adjustments were required over the use of APC and APC-Cy7 in simultaneous labeling. This is unsurprising given the
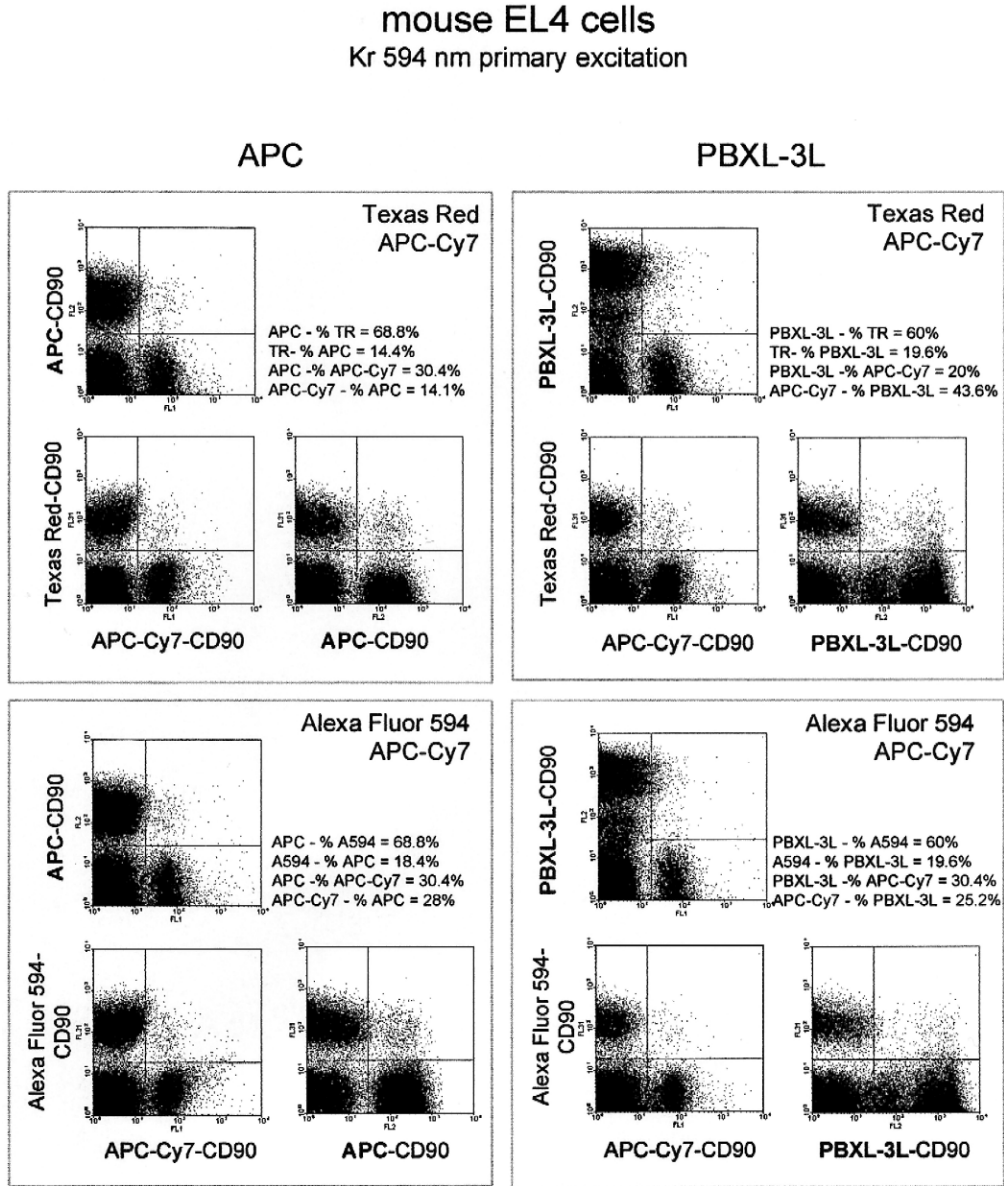

Fig. 9. Multicolor analysis with yellow 594 nm-excited probes and PBXL-3L. Mouse EL4 cells were labeled with biotin-anti-CD90 followed by streptavidin conjugated with either APC, PBXL-3L, Texas Red, Alexa Fluor 594 dye or APC-Cy7. Cell mixtures of APC (left panels, top and bottom) or PBXL-3L (right panels, top and bottom) and Texas Red and APC-Cy7 (top panels) or Alexa Fluor 594 dye (bottom panels) were prepared and analyzed on a hybrid FACStar with HeNe 594 nm (4.5 mW) excitation. Data are displayed as cytograms with all two-color combinations, with all color compensation percentages shown.
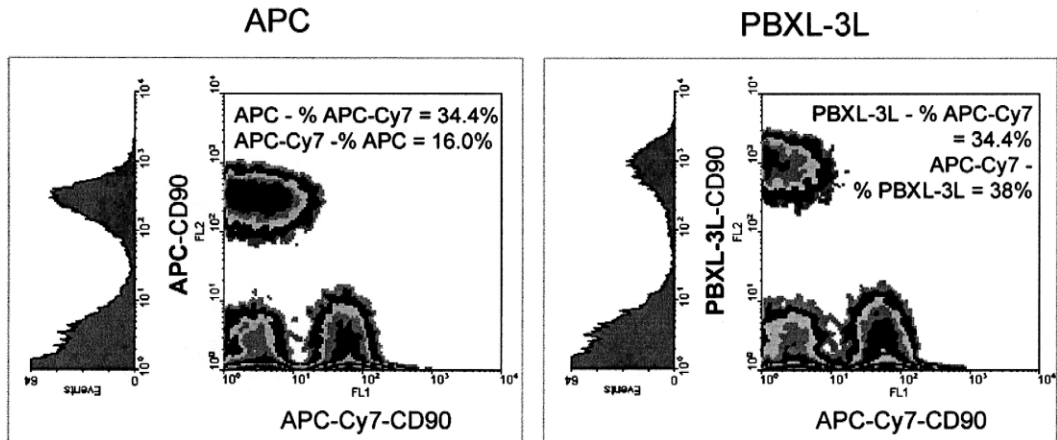
Fig. 10. Multicolor analysis with yellow 612 nm-excited probes and PBXL-3L. Mouse EL4 cells were labeled with biotin-anti-CD90 followed by streptavidin conjugated with either APC, PBXL-3L, or APC-Cy7. Cell mixtures of APC (left panel) or PBXL-3L (right panel) and APC-Cy7 were prepared and analyzed on a hybrid FACStar with HeNe 612 nm (4.5 mW) excitation. Data are displayed as cytograms with all two-color combinations, with all color compensation percentages shown. APC and PBXL-3L labeling is shown at left for isotype control (open peaks) and specific labeling (filled peaks).

broader emission bandwidth of PBXL-3L, and again was not excessively high. As above, APC and PBXL-3L functioned equally well with FITC and PE labeling in three-color experiments.

In Fig. 3, it was demonstrated that Kr 568 nm excitation gave adequate (although not optimal) excitation of PBXL-3L. The Kr 568 nm line is useful for exciting a number of important fluorochromes with emission bandwidths in the orange range, including lissamine rhodamine, Texas Red, Alexa Fluor 568 and 594 dyes (brighter, more photostable versions of lissamine rhodamine and Texas Red) and the cryptomonad algal phycobiliprotein CryptoFluor-5. It was therefore determined whether PBXL-3L emission was compatible with these dyes using the CD90-labeled EL4 cell mixtures described for Fig. 7. Using Kr 568 nm excitation (Fig. 8), both APC and PBXL-3L signals could be separated from lissamine rhodamine, Alexa Fluor 568 dye, Alexa Fluor 594 dye and CryptoFluor-5 using a 640 LP dichroic. A somewhat higher compensation subtraction for PBXL-3L was again required but was not excessive.

The lower power HeNe 594 and 612 nm lasers, used for data shown in Fig. 3, are seeing increasing usage in flow cytometry. These low power lasers can also be used to excite more than one fluorochrome with suitable selection of fluors. These lasers showed the strongest signal-to-noise ratio for PBXL-3L excitation. Texas Red and Alexa Fluor 594 dye are optimally excited at 594 nm; the APC-Cy7 tandem conjugate is also useful at this wavelength. PBXL-3L was therefore tested for compatibility with simultaneous labeling with Texas Red or Alexa Fluor 594 and APC-Cy7 using the HeNe 594 nm laser as primary excitation source (as described in Fig. 3). Texas Red or Alexa Fluor 594 signals were separated from APC or PBXL-3L and APC-Cy7 using a 640 LP dichroic; APC or PBXL-3L and APC-Cy7 signals were separated using a 690 LP (Fig. 9). PBXL-3L was again compatible with these two fluorochromes for three-color analysis using a single yellow laser. PBXL-3L was also compatible with APC-Cy7 using a HeNe 612 nm laser (Fig. 10).

4. Discussion

The data presented here show that the PEG spacer arm construct of the chemically stabilized phycobili-

some PBXL-3 (designated PBXL-3L) is an effective immunophenotyping fluorochrome for flow cytometry. PBXL-3L was more sensitive than APC for the immunodetection of weak surface markers, both in cell lines and in primary lymphoid cells. PBXL-3L was also found to be spectrally compatible with a wide variety of commonly used fluorescent tags, including: (1) the blue-green excited fluorochromes FITC, PE, PE-Cy5, PE-Cy7 and PerCP-Cy5.5, (2) the yellow-orange excited fluorochromes Crypto-Fluor-5, Texas Red, lissamine rhodamine, Alexa Fluor 568 dye and Alexa Fluor 594 dye, and (3) the red-excited tandem conjugate APC-Cy7. PBXL-3L can thus be substituted for APC in situations where greater detection sensitivity is desired.

Another interesting characteristic of the PBXL-3 phycobilisome was its observed high level of fluorescence intensity when excited with low power laser sources. PBXL-3L possessed an optimal signal-to-noise ratio when excited with the lowest power lasers, including HeNe 594 and 612 nm lasers emitting at less than 5 mW measured output. Although not emitting at the PBXL-3 excitation maxima, a 5 mW red diode laser gave among the highest signal-to-noise ratios for all sources tested. This high fluorescence intensity is not surprising given the multiple phycobiliprotein-containing structure of the PBXL dyes, suggesting that they would retain their native energy transfer efficiency level.

The high fluorescence intensity of the PBXL dyes may make them particularly applicable to modern flow cytometers. A major trend in flow cytometry instrument development is the incorporation of high-efficiency, air-cooled lasers with lower power outputs (Shapiro, 1995). Replacing large, expensive, water-cooled lasers with these smaller, cheaper light sources will make flow cytometers smaller, more rugged, less expensive, less demanding of maintenance and more reliable. Commercial benchtop instruments now make use of several low power laser sources, including both red diode (635 nm), diode-pumped solid state lasers (532 nm) and small HeNe lasers (including the 543 nm "GreNe" lasers)(Shapiro, 1995). The 594 and 612 nm HeNe lasers used in this study are other examples of small lasers that will see expanded use in flow cytometry. Dedicated microbead flow cytometers (including the LabMAP™ system from Luminex, Austin, TX) are in particular

making use of small laser sources, as are recently developed portable instruments for field usage (including the OptiFlow MicroCyte™ portable cytometer). Carefully designed optics can produce detection sensitivities approaching large instruments with more powerful laser sources. Extremely efficient fluorochromes, such as the PBXL dyes, will be particularly useful in these modern flow cytometers.

References

Beavis, A.J., Pennline, K.J., 1996. ALLO-7: a new fluorescent tandem dye for use in flow cytometry. Cytometry 24, 390.

Biggins, J., Bruce, D., 1989. Regulation of excitation energy transfer in organisms containing phycobilins. Photosynth. Res. 20, 1.

Brimble, S., Bruce, D., 1989. Pigment orientation and excitation energy transfer in *Porphyridium cruentum* and *Synechococcus* sp. PCC 6301 cross-linked in light state 1 and light state 2 with glutaraldehyde. Biochim. Biophys. Acta 973, 315.

Cubicciotti, R., 1997. Phycobilisomes, derivatives, and uses therefor. US Patent No. 5,695,990.

Gagliano, A.G., Hoarau, J., Breton, J., Geacintov, N.E., 1985. Orientation of pigments in phycobilisomes of *Porphyridium* sp. Lewin. A linear dichroism study utilizing electric and gel orientation methods. Biochim. Biophys. Acta 808, 455.

Gantt, E., Lipschultz, C.A., 1972. Phycobilisomes of *Porphyridium cruentem*: I. Isolation. J. Cell Biol. 54, 313.

Gantt, E., Lipschultz, C.A., 1973. Energy transfer in phycobilisomes from phycoerythrin to allophycocyanin. Biochim. Biophys. Acta 292, 858.

Gantt, E., Lipshultz, C.A., Grabowski, J., Zimmerman, B.K., 1979. Phycobilisomes from blue-green and red algae. Plant Physiol. 63, 615.

Glazer, A., 1984. Phycobilisome: a macromolecular complex specialized for light energy transfer. Biochim. Biophys. Acta 768, 29.

Glazer, A.N., Stryer, L., 1983. Fluorescent tandem phycobiliprotein conjugates. Emission wavelength shifting by energy transfer. Biophys. J. 43, 383.

Landsdorp, P.M., Smith, C., Safford, M., Terstappen, L.W., Thomas, T.E., 1991. Single laser three color immunofluorescence staining procedures based on energy transfer between phycoerythrin and cyanin 5. Cytometry 12, 723.

MacColl, R., Guard-Friar, D., 1987. Phycobiliproteins. CRC Press, Boca Raton, pp. 73–93.

Morseman, J., Moss, M.W., Zoha, S.J., Allnutt, F.C.T., 1999. PBXL-1: a new fluorochrome applied to detection of proteins on membranes. BioTechniques 26, 559.

Morseman, J., Zeng, X., Rogers, Y.-H., Allnutt, F.C.T., 2000. Direct fluorescent detection of biotinylated oligonucleotides on glass slides using streptavidin labeled with PBXL-1 or phycoerythrin. Lumin. Forum 6, 4.

Oi, V.T., Glazer, A.N., Stryer, L., 1982. Fluorescent phycobilipro-

tein conjugates for analyses of cells and molecules. J. Cell Biol. 93, 981.

Roederer, M., Bigos, M., Nozaki, T., Stovel, R.T., Parks, D.R., Herzenberg, L.A., 1995. Heterogenous calcium flux in peripheral T cell subsets revealed by five-color flow cytometry using log-ratio circuitry. Cytometry 21, 187.

Roederer, M., Kantor, A.B., Parks, D.R., Herzenberg, L.A., 1996. Cy7PE and Cy7APC: bright new probes for immunofluorescence. Cytometry 24, 191.

Roederer, M., De Rosa, S., Gerstein, R., Anderson, M., Bigos, M., Stovel, R., Nozaki, T., Parks, D., Herzenberg, L., Herzenberg, L., 1997. 8-color, 10-parameter flow cytometry to elucidate complex leukocyte heterogeneity. Cytometry 29, 328.

Shapiro, H.M., 1995. Practical flow cytometry. Wiley, New York, pp. 277–280.

Waggoner, A.S., Ernst, L.A., Chen, C.H., Rechtenwald, D.J., 1993. PE-CY5. A new fluorescent antibody label for three-color flow cytometry with a single laser. Ann. N. Y. Acad. Sci. 677, 185.

Yakamura, G., Glazer, A.N., Williams, R.C., 1980. Molecular architecture of a light-harvesting antenna. Comparison of wild type and mutant *Synechococcus* 6301 phycobilisomes. J. Biol. Chem. 255, 11104.

Yeh, S.W., Ong, L.J., Clark, J.H., Glazer, A.N., 1987. Fluorescence properties of allophycocyanin and a crosslinked allophycocyanin trimer. Cytometry 8, 91.

Zhang, Y., Chen, X., Liu, J., Pang, S., Shi, D., Zeng, C., Zhou, B., 1999. A new model of phycobilisome in *Spirulina platensis*. Sci. China, Ser. C: Life Sci. 41, 74.

Zoha, S., Ramnarain, S., Allnutt, F.C.T., 1998. Ultrasensitive direct fluorescence immmunoassay for thyroid stimulating hormone. Clin. Chem. 44, 2045.